Climate–vegetation control on the diurnal and seasonal variations of surface urban heat islands in China

2016 Environ. Res. Lett. 11 074009

(http://iopscience.iop.org/1748-9326/11/7/074009)

Environmental Research Letters

LETTER

Climate–vegetation control on the diurnal and seasonal variations of surface urban heat islands in China

Decheng Zhou[1], **Liangxia Zhang**[1], **Dan Li**[2], **Dian Huang**[3] **and Chao Zhu**[4]

[1] Jiangsu Key Laboratory of Agricultural Meteorology, College of Applied Meteorology, Nanjing University of Information Science and Technology, Nanjing 210044, People's Republic of China
[2] Department of Earth and Environment, Boston University, Boston, Massachusetts 02215, USA
[3] College of Urban and Environmental Sciences, and Key Laboratory for Earth Surface Processes of the Ministry of Education, Peking University, Beijing 100871, People's Republic of China
[4] Nanjing Institute of Environmental Sciences of the Ministry of Environmental Protection of PR China, Nanjing, Jiangsu, 210042, People's Republic of China

E-mail: zhoudc@nuist.edu.cn

Keywords: urbanization, temporal variation, land surface temperature, MODIS, urban heat island

Supplementary material for this article is available online

OPEN ACCESS

RECEIVED
1 March 2016

REVISED
20 April 2016

ACCEPTED FOR PUBLICATION
21 June 2016

PUBLISHED
8 July 2016

Abstract

Remotely sensed surface urban heat islands (UHIs) have gained considerable interest in recent decades due to the easy access and the wall-to-wall coverage of satellite products. The magnitude or intensity of surface UHIs have been well documented at regional and global scales, yet a systematic evaluation of the temporal variability over large areas is still lacking. In this study, the diurnal and seasonal cycles of surface UHI intensities (SUHIIs) in China are examined using Aqua/Terra MODIS data from 2008 to 2012. Results show that the mean annual SUHIIs varied greatly in a diurnal cycle, characterized by a positive day-night difference (DND) in Southeast China and the opposite in Northeast and Northwest China. Also, the SUHIIs differed dramatically in a seasonal cycle, indicated by a positive summer-winter difference (SWD) in the day and a negative SWD at night, accompanied by the highly diverse DNDs across seasons and geographic regions. Northwest and Northeast China overall showed the largest DND and SWD (>3 °C), respectively. These diurnal and seasonal variations depend strongly on local climate-vegetation regimes, as indicated by a strong positive correlation between DND and precipitation (and air temperature) and a negative relationship between DND and vegetation activity across cities and seasons. In particular, SHUIIs were quadratically correlated with the mean annual precipitation across space, suggesting that there might be a threshold in terms of the effects induced by local background climate. Our findings highlight the importance of considering the temporal variability of UHIs for more accurate characterization of the associated ecological and social-economic consequences.

1. Introduction

Urbanization, broadly defined as the process of urban land expansion and demographic shift from rural to urban areas, represents the most visible, indispensable, and pervasive anthropogenic modification to the Earth system (Grimm *et al* 2008, Seto *et al* 2011, Wu 2014). About 54% of the world's population resides in urban areas in 2014, and this number is projected to become 66%-with more than 6 billion urban inhabitants by 2050 (United Nations 2015). The global urban area is expanding at twice its population growth rate (Angel *et al* 2011) and may triple the area of 2000 in 2030 if the trend continues (Seto *et al* 2012).

Although there is no doubt that urban areas will play an irreplaceable role in achieving a sustainable future for human societies (Wu 2014), they have been causing many environmental issues (Grimm *et al* 2008). The urban heat island (UHI) effect, which refers to the temperature rise in urban areas than surrounding suburban/rural areas (Howard 1833, Manley 1958, Oke 1973), is a good example. UHIs can alter

the eco-environments such as vegetation activity (Imhoff *et al* 2004, Zhou *et al* 2014a, 2016), biodiversity (Reid 1998), water and air quality (Grimm *et al* 2008), and local climate (Arnfield 2003, Shepherd 2005, IPCC 2014). They can also seriously affect human health and air quality resulting in increases in morbidity and mortality (Patz *et al* 2005, Gong *et al* 2012, Kolokotroni *et al* 2012). Worse still, these impacts can be more serious under a changing climate (Patz *et al* 2005, Li and Bou-Zeid 2013, IPCC 2014, Zhao *et al* 2014, Li *et al* 2015). Therefore, understanding and mitigating UHIs have gained strong interest from scientists and urban planners and have been the subject of active research (Kolokotroni *et al* 2012, Li and Bou-Zeid 2013, 2014, Li *et al* 2014, 2015, Zhao *et al* 2014).

The UHI effect, typically defined as the temperature difference between urban and suburban/rural areas, can be categorized into two broad types based on the measurement technique. The first is the air UHI calculated from weather stations (Peterson 2003, Fast *et al* 2005, Chow and Roth 2006) and the second is the surface UHI often estimated from thermal infrared remote sensing data (Voogt and Oke 2003). These two UHIs are closely related but can be significantly different in terms of magnitude and spatial-temporal pattern (Arnfield 2003, Jin and Dickinson 2010). Studies on air UHIs are more extensive due to the availability of weather station data. However, the surface UHIs have gained increasing attention in recent decades as the remote sensing technique becomes mature and widely used in earth sciences (Jin and Dickinson 2010, Zhang *et al* 2010, Peng *et al* 2012).

The magnitude or intensity of surface UHI has been studied in North America (Zhao *et al* 2014. Imhoff *et al* 2010), Europe (Zhou *et al* 2013), Asia (Tran *et al* 2006, Zhou *et al* 2014b, 2015), and the world (Jin *et al* 2005, Zhang *et al* 2010, Peng *et al* 2012, Clinton and Gong 2013). However, the temporal variability remains poorly understood over large areas. On one hand, most previous efforts focused on the overall day-night or summer-winter differences of SUHIIs (Tran *et al* 2006, Imhoff *et al* 2010, Peng *et al* 2012, Clinton and Gong, 2013, Zhou *et al* 2014b) and didn't explore the spatial heterogeneities in detail. This might result in biases in their reported temporal trends of SUHIIs across large areas. For example, Peng *et al* (2012) concluded that the SHUIIs were clearly larger in the day than at night, whereas Clinton and Gong (2013) emphasized that globally the magnitude of SHUIIs was similar in the day and night. On the other hand, factors such as the reduction of latent heat flux and the increases of ground heat storage and anthropogenic heat releases are well known to be responsible for the UHI effect (Oke 1982, Arnfield 2003), yet the relationship between SUHIIs (in particular their temporal pattern) and the background climate-vegetation condition is still not well documented. A recent study suggested strong contributions of local background climate to UHIs (Zhao *et al* 2014), which only focused on the annual mean UHIs and neglected the role of vegetation. Consequently, our study aims to improve our understanding of the temporal variability of surface UHIs and the relations with the background climate and vegetation.

Located in the East Asian monsoon region, China has complex zonal climatic variations from the tropical to subarctic/alpine and from rain forest to desert (Wu *et al* 2005). In parallel, it has been experiencing the rapidest urbanization in the world in recent decades (Seto *et al* 2011, United Nations 2015), which is also different from other developed or developing countries (Zhao *et al* 2015a, 2015b). Thus, China is ideal for the investigation of UHI effects at a regional level. In this study, we analyzed the SUHIIs in 32 major cities in China distributed in different climatic zones using the cloud-free Moderate Resolution Imaging Spectroradiometer (MODIS) in conjunction with Landsat Thematic Mapper (TM) and Enhanced Thematic Mapper Plus (ETM +) data between 2008 and 2012. Our main objectives are to (1) systematically evaluate the diurnal and seasonal cycles of SUHIIs, and (2) examine their relationships with background climate and vegetation activities. The inter-annual variability of SUHIIs is not examined here.

2. Data and methods

2.1. Data

All 32 cities analyzed in this study are municipalities and provincial capitals except Shenzhen, which was included because it is China's first special economic zone established in 1978 and is now considered as one of the fastest growing cities (figure 1). Most cities are mainly surrounded by cultivated land, with a few cases by forests (e.g., Hangzhou and Fuzhou) or grassland (Lhasa). Land cover maps within the administrative boundary of each city were derived from the cloud-free Landsat TM (downloaded free from http://www.usgs.gov/) with a resolution of 30 m for the year 2010. The gap-filled Landsat ETM+ Scan Line Corrector (SLC)-off products (obtained free from http://www.gscloud.cn/) were used for a few cities that do not have the TM data. The scan gaps of ETM+ images were filled using a local linear histogram matching techni que (Storey *et al* 2005). Around 85 scenes of images spanning 2009–2011 were used to extract the extent of urban land for all the cities in this study (supporting information table S1). The land covers were classified into four types (i.e., cropland, built-up land, water body, and others) using the maximum likelihood classification approach (Zhao *et al* 2015a). The built-up land consisted of the impervious surfaces of cities, towns (e.g., roads, parking lots, and buildings), includ ing residential, commercial, industrial, and transporta tion spaces. The accuracy of the classified product was assessed using the high-resolution images and pictures

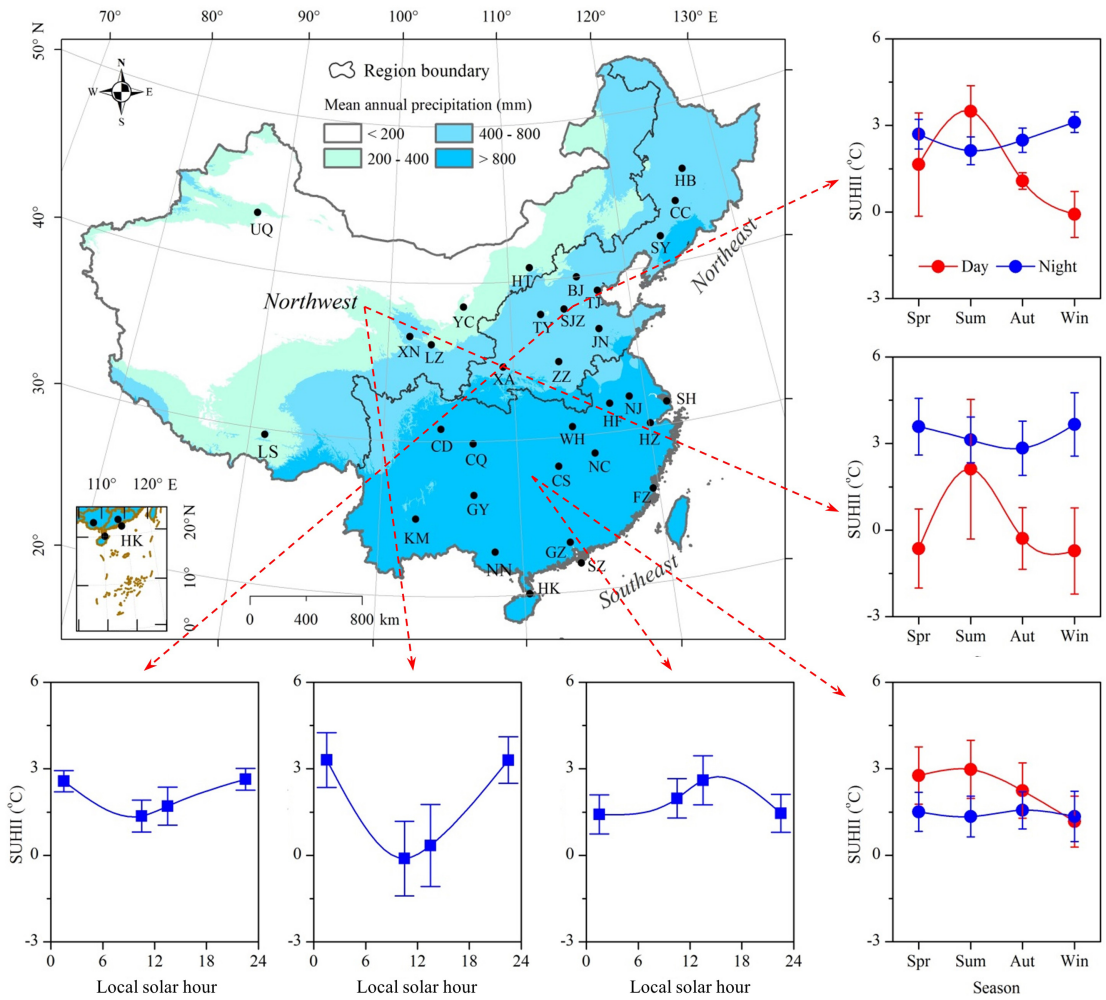

Figure 1. Locations of the 32 major Chinese cities (with the background indicating the mean annual precipitation), and the diurnal and seasonal variations of surface urban heat island intensity (SUHII) in the three climatic regions (i.e., Northeast, Northwest, and Southeast) of China. Spr, Sum, Aut, and Win represent spring, summer, autumn, and winter seasons, respectively. BJ: Beijing; CC: Changchun; CS: Changsha; CD: Chengdu; CQ: Chongqing; FZ: Fuzhou; GZ: Guangzhou; GY: Guiyang; HK: Haikou; HZ: Hangzhou; HB: Harbin; HF: Hefei; HT: Hohhot; JN: Jinan; KM: Kunming; LZ: Lanzhou; LS: Lhasa; NC: Nanchang; NJ: Nanjing; NN: Nanning; SH: Shanghai; SY: Shenyang; SZ: Shenzhen; SJZ: Shijiazhuang; TY: Taiyuan; TJ: Tianjin; UQ: Urumqi; WH: Wuhan; XA: Xi'an; XN: Xining; YC: Yinchuan; ZZ: Zhengzhou. Map was generated using ArcGIS 9.3 (www.esri.com/software/arcgis).

incorporated in Google Earth Pro. The accuracies, measured by Kappa coefficients, were generally larger than 0.80 for all cities considered here. Further details on land cover data can be found in Zhao *et al* (2015a).

Remotely sensed LST was used to characterize the UHI effect. The LST data for each city from 2008 to 2012 at four local solar hours (i.e., 01:30, 10:30, 13:30 and 22:30) were obtained from Aqua/Terra MODIS 8-day composite products with a spatial resolution of 1 km (MYD11A2 and MOD11A2). The LST was retrieved from clear-sky (99% confidence) observations using a generalized split-window algorithm (Wan and Dozier 1996). It has been widely validated with biases less than 1 K (Wan 2008) and the mean absolute differences (relative to *in situ* measurements) less than 5% in urban areas (Rigo *et al* 2006).

Digital Elevation Model (DEM) at a 3 arc-second (approximately 90 m) spatial resolution from the Space Shuttle Radar and Topography Mission (SRTM) was utilized to exclude the altitude effect. The version-5 Aqua MODIS enhanced vegetation index (EVI) from 2008 to 2012 (MYD13A2, 16-day composite, 1 km spatial resolution) was used to represent the vegetation condition for each city. Moreover, monthly climate data of precipitation and air temperature from Chinese Meteorological Observations (downloaded from http://cdc.cma.gov.cn/) for the period of 2008 and 2012 were utilized to represent the background cli mate for each city. One meteorological station located within the urban area or nearby suburb for each city was used. This may introduce some biases due to the possible urbanization and topographical effects, but should not alter the spatial pattern of the background climate across cities significantly (Arnfield 2003).

2.2. Analysis

In this study, we defined the surface UHI intensity (i.e., SUHII) as the LST difference between urban and

far-away rural areas (supporting information figure S1). Following the convention (Schneider *et al* 2009), areas dominated by high-density built-up land (>50%) were defined as urban areas. Specifically, the urban areas were defined by three steps. First, a built-up intensity (BI) map was generated from each urban coverage map using a 1 km × 1 km moving window, which matches the pixel size of MODIS LST data. Second, a 50% threshold of BI was used as a criterion to separate the BI maps into high- and low-intensity built-up land. Finally, the high-intensity built-up polygons were aggregated to delineate the urban border with an aggregation distance of 2 km, which is sufficient to include the scattered and most adjacent high-intensity built-up patches into the urban class. The urban areas obtained by this method in 2010 ranged from 47.6 km^2 (Lhasa) to 2350.6 km^2 (Tianjin). The rural areas were then defined as the buffer zone 40–45 km away from urban perimeter (Imhoff *et al* 2010) and outside the UHI footprint (Zhou *et al* 2015).

We mapped urban and rural areas for each city in 2010 and assumed that they can be used to represent conditions in 2008–2012. Water body pixels or those with an elevation more than 50 m above the highest point of the urban area were excluded from this analysis. The diurnal (at 01:30, 10:30, 13:30 and 22:30 local solar hour) and seasonal SUHIIs were then calculated over the period 2008–2012 for each city individually. Spring, summer, autumn, and winter were defined as the periods from March to May, June to August, September to November, and December to February, respectively. The day-night difference (DND) and the summer-winter difference (SWD), defined as the SUHII differences between day (average of the observations at 10:30 and 13:30 local solar hour) and night (average of the observations at 22:30 and 1:30 local solar hour) and between summer and winter, respectively, were also used. Since the SUHII may vary inter-annually due to climate variability, urban development, and/or varying data quality, the SUHII estimates over the period 2008–2012 were averaged to provide a general picture for each city.

To demonstrate the SUHII variations across climatic regimes, those 32 major cities were grouped into three regions according to local climatic conditions (downloaded from the global climate database at http://www.worldclim.org/) (figure 1) (Wu *et al* 2005): Northeast China (Beijing, Changchun, Harbin, Jinan, Shenyang, Shijiazhuang, Taiyuan, Tianjin, Xi'an, Zhengzhou), Northwest China (Hohhot, Lanzhou, Lhasa, Urumqi, Xining, and Yinchuan), and Southeast China (Changsha, Chengdu, Chongqing, Fuzhou, Guangzhou, Guiyang, Haikou, Hangzhou, Hefei, Kunming, Nanchang, Nanjing, Nanning, Shanghai, Shenzhen, and Wuhan). Northeast China has typical semi-humid temperate climate, with the mean annual precipitation (MAP) less than 800 mm and larger than 400 mm. Northwest and Southeast China have typical arid temperate (MAP $\leqslant$ 400 mm) and humid hot (MAP $>$ 800 mm) climates, respectively. Analyses in the three regions were conducted separately.

The EVI differences (ΔEVI) between urban and rural areas and two climate variables (precipitation and air temperature) were used to examine possible climate and vegetation effects on the SUHII patterns. First, the Spearman's correlation coefficients between mean annual SUHII or DND and the three variables across cities were calculated using Matlab (http://www.mathworks.co.uk/products/matlab/). The linear, logistic, and quadratic regression analyses were further performed to check the form of their relationships. The goodness of the fit was evaluated by the corrected Akaike Information Criterion (AICc) (Motulsky and Christopoulos 2004, Zhou *et al* 2014a):

$$AIC_c = N * \ln\left(\frac{RSS}{N}\right) + 2K + \frac{2K(k+1)}{N-K-1}$$

where N is the number of data points, K is the number of parameters fit by the regression plus 1, and RSS is the residual sum of squares of the model. When comparing two models, the model with a lower AIC_c score is considered better. Furthermore, the Spearman's correlation coefficients between the monthly SUHII or DND and the three variables averaged over different regions of China were calculated to explore the impacts of local climate and vegetation on the SUHII's seasonality.

Because SUHII may vary by the definition, we first quantified the SUHII using another two commonly used definitions (Peng *et al* 2012, Zhou *et al* 2014b) in order to test if the results are sensitive to its definition (see detailed method in supporting information figure S1). Consistent with previous studies (Schwarz *et al* 2011, Zhou *et al* 2015), the SUHII varied significantly by definitions. For example, the SUHIIs defined in this study were much larger than those defined as the temperature difference between urban and surrounding suburban areas. The sign of the SUHII could be even reversed (supporting information figure S2). However, the diurnal and seasonal patterns were similar across these definitions (supporting information figure S3). This suggests that although the magnitude of SUHII is definition-dependent, the temporal pattern is more likely controlled by other factors. Unraveling these factors is exactly the motivation of this study.

Moreover, we estimated the SUHIIs in a longer time period in order to examine whether the results are influenced by the temporal scale. As shown in figure S4, the diurnal and seasonal variations of SUHIIs averaged over 2003–2012 are very consistent with those in our study period of 2008–2012, indicating that the period we selected can represent the general patterns of SUHIIs for all 32 cities.

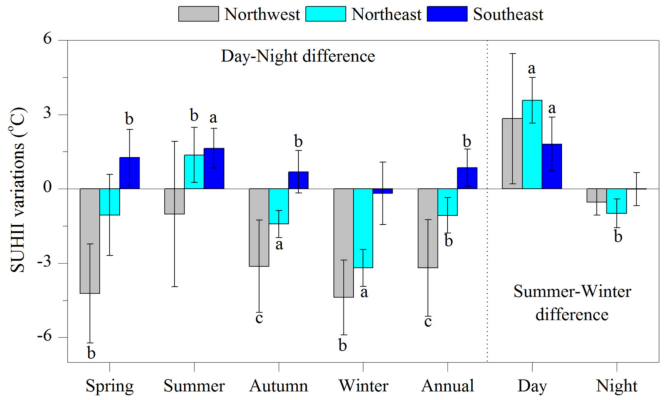

Figure 2. Day-night differences and summer-winter differences of SUHIIs in different regions of China. The average of the observations at 10:30 and 13:30 local solar hours and that at 22:30 and 1:30 local solar hours were used to represent daytime and night SUHIIs, respectively. (a), (b), (c), indicate that the differences are significant at 0.001, 0.01, and 0.05 levels, respectively.

3. Results

3.1. Diurnal and seasonal variations of SUHIIs

The SUHIIs varied substantially in a diurnal cycle for all 32 cities, with contrasting patterns by region (figure 1). The SUHII averaged in Northwest China was significantly lower in the day than at night, with annual mean ranging from $-0.1 \pm 1.3\,^{\circ}C$ at 10:30 local solar time to $3.3 \pm 0.9\,^{\circ}C$ at 1:30 local solar time. The same happened in Northeast China, but with a smaller difference between day and night. The day-night difference (i.e., DND) averaged in Northeast China was one-third of that in Northwest China (-1.1 ± 0.7 versus $-3.2 \pm 1.9\,^{\circ}C$) (figure 2). In contrast, the daytime SUHII was clearly larger than the nighttime SUHII for Southeast China, indicated by a positive DND of $0.85 \pm 0.7\,^{\circ}C$ (figures 1 and 2). Results for individual cities are shown in the supporting information (figure S5).

Large seasonal variations of SUHII were observed during daytime in China (figure 1). Overall, daytime SUHIIs were the strongest in summer and the weakest in winter for all three regions of China (figure 1). The daytime summer-winter differences (SWDs) reached a maximum of $3.6 \pm 0.9\,^{\circ}C$ in Northeast China, followed by Northwest China ($2.8 \pm 2.6\,^{\circ}C$) and Southeast China ($1.8 \pm 1.1\,^{\circ}C$) (figure 2). Results for individual cities are provided in the supplementary information (figure S6). Interestingly, the SUHII maximized in the spring season in a few cities, such as Xi'an, Nanjing, and Shanghai. In contrast, the nighttime SUHIIs fluctuated only slightly by season (figure 1). The nighttime SUHIIs were maximum in winter and minimum in summer/autumn for Northeast and Northwest China, while remained stable in Southeast China. More specifically, the SWDs were $-1.0 \pm 0.6\,^{\circ}C$ in Northeast China, $0.5 \pm 0.5\,^{\circ}C$ in Northwest China, and $-0.01 \pm 0.7\,^{\circ}C$ in Southeast China (note results in Northwest and Southeast China are not statistically significant). As a result, the diurnal cycles of SUHIIs differed significantly by season and region (figure 2). The DND was negative in all seasons and particularly during winter in Northwest China. Comparatively, it was positive in summer and negative in the other seasons in Northeast China. In Southeast China, it was negative in winter and positive in the other seasons.

3.2. Relationships between SUHIIs and climate-vegetation factors

The mean annual SUHII across cities were significantly and positively correlated with the mean annual precipitation (MAP) and air temperature (MAT) during the daytime, with the Spearman's coefficients (r) of 0.58 and 0.52 ($p < 0.01$), respectively. However, the opposite correlations were observed at night (figure 3). As a result, the mean annual DND was most closely and positively linked to MAP ($r = 0.79$) and MAT ($r = 0.76$). The corrected Akaike Information Criterion (AICc) analysis further showed that the relationship between SUHII and MAT was linear but that between SUHII and MAP was in a quadratic form. In particular, those relationships held regardless of SUHII definitions (supporting information, figure S7). Moreover, the $\triangle$EVI was negatively and significantly ($p < 0.05$) correlated with the daytime SUHII as well as the DND. In contrast, it was positively but statistically insignificantly correlated with the nighttime SUHII.

The seasonal changes of the SUHIIs were also closely related to the fluctuations of local climate and vegetation activity, especially during the daytime. As illustrated in figure 4, the monthly mean daytime SUHIIs were negatively correlated with monthly mean ΔEVI in all regions, especially in Northeast China ($r = 0.95$, $p < 0.001$). Meanwhile, they were positively and significantly ($p < 0.01$) correlated with the monthly precipitation or air temperature in all regions (figure 4). The relationships between DNDs and those variables were generally similar to that of daytime

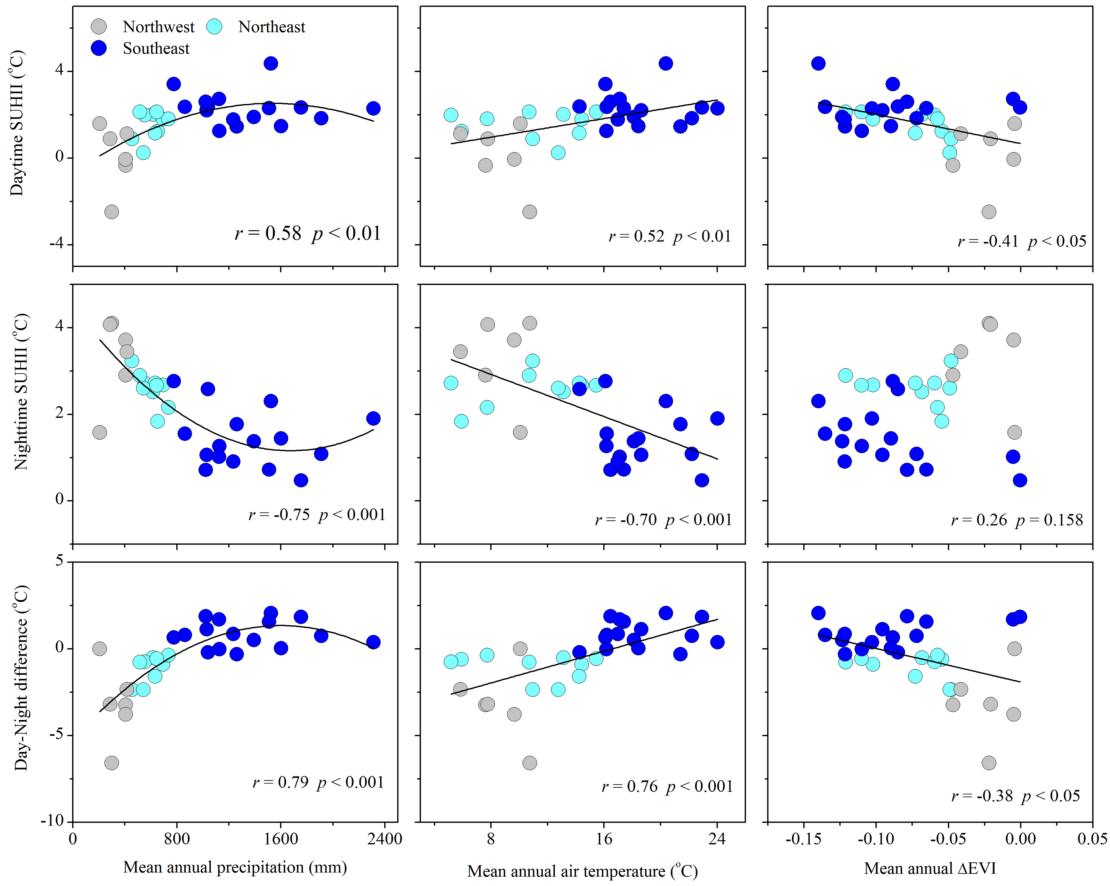

Figure 3. Relationship between mean annual SUHIIs and climate-vegetation factors across China's 32 major cities, with the *r* indicating the Spearman's correlation coefficient. The linear, logistic, and quadratic regressions were used to examine the relationship. The goodness of the fit was evaluated by the corrected Akaike Information Criterion (AICc), and only the best fitted lines were shown in the graph. ΔEVI means differences of enhanced vegetation index between urban and rural areas.

SUHIIs. In contrast, the overall reverse correlations were observed at night, but the relationship was only statistically significant in Northeast China.

4. Discussion

4.1. Diurnal and seasonal cycles of SUHIIs in China

Our results indicated that the SUHIIs varied substantially in a diurnal cycle, with contrasting patterns in different regions of China (figure 1). This diurnal variability is attributed to the different UHI energetics between day and night (Oke 1982, Peng *et al* 2012, Zhou *et al* 2014b). The formation of UHI during the day is largely driven by more sensible heat and less latent heat owing to the reduction of green space in urban areas. Comparatively, the nighttime UHI typically results from more energy storage in urban areas (trapped during the day and released at night). The annual mean SUHII was lower in the day (than at night) over northern China (especially in Northwest China) because the reference rural areas in north part warm faster in the day (less vegetation activity) and cool faster (smaller soil heat capacity) at night under the drier climate. On the other hand, the annual mean SUHII was higher in the day over Southeast China because the reference rural areas warm slower in the day and cool slower at night. These patterns differed slightly from the findings in the continental United States by Imhoff *et al* (2010). They found that the daytime SUHIIs were larger than the nighttime SUHIIs in all the regions except arid biomes. The reason for the discrepancy was not clear but might be related to different land-use patterns. For example, the rural areas of the United States were generally covered by a higher portion of forests (Imhoff *et al* 2010) as compared to the rural areas of China that were overwhelmingly dominated by cropland (Zhou *et al* 2014a). The cropland is characterized by larger surface albedo than forests that could strengthen the nighttime SUHII by reducing the energy absorption during the day for later releasing (Jin *et al* 2005). Our results were also different from many theoretical (Oke 1982, Arnfield 2003), observational (Huang *et al* 2008), and modeling (Miao *et al* 2009) studies showing that air UHIs were more intensive at night under the calm air and clear sky conditions. The disparity can be attributed to the differences between land surface temperature (i.e., LST) and near-surface air temperature (Arnfield 2003, Voogt and Oke 2003, Jin and Dickinson 2010) and their different

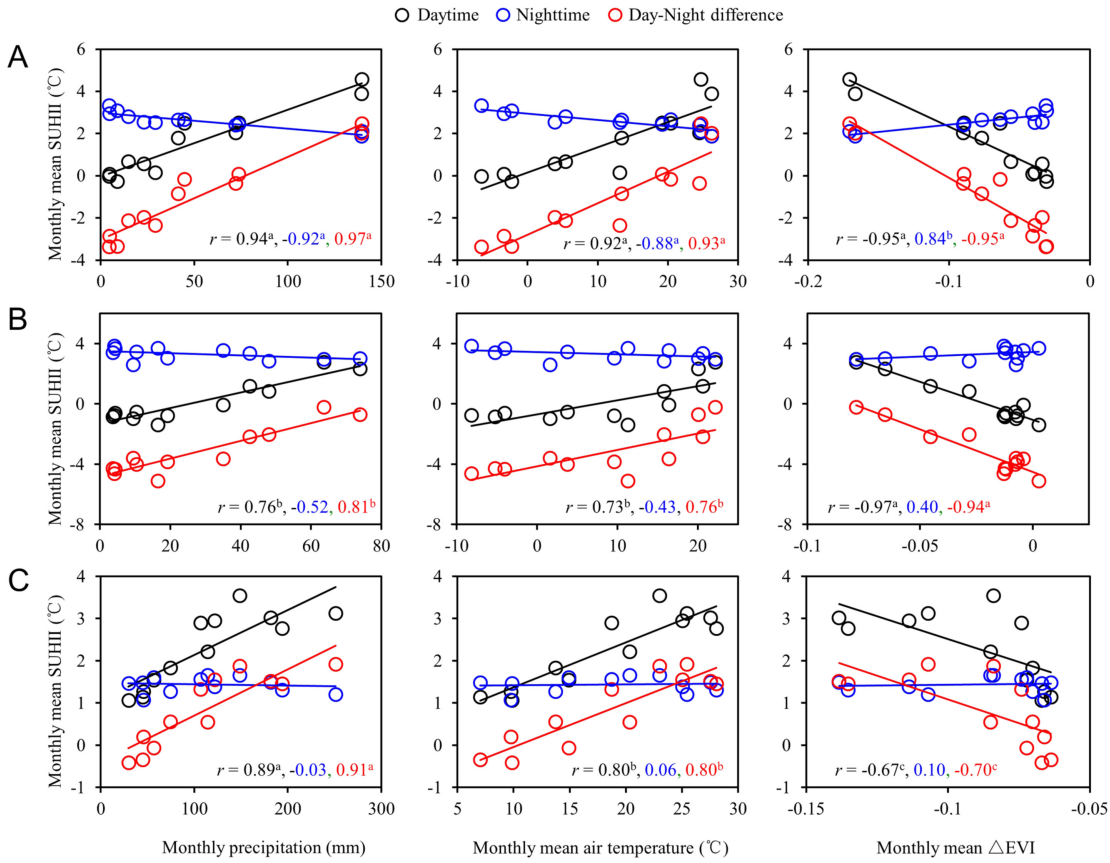

Figure 4. Relationship between monthly SUHIIs and climate-vegetation factors averaged over Northeast China (A), Northwest China (B), and Southeast China (C). The *r* values for the day (black), night (blue), and day-night difference (red) were showed in each figure panel. (a), (b) and (c) indicate that the correlations are significant at 0.001, 0.01, and 0.05 levels, respectively.

measurement techniques. Remotely sensed LST is determined by both surface properties (soil, vegetation, etc) and atmosphere conditions (water vapor, clouds, etc), while the air temperature is mainly determined by the near-surface air conditions. These two temperatures are closely correlated but can differ in terms of magnitude and possibly the spatiotemporal pattern depending on land and/or sky conditions (Jin and Dickinson 2010). Larger surface UHIs are observed during daytime (e.g., southeast China) since the land surface heats and cools more rapidly than air (Roth *et al* 1989).

Large and asymmetric seasonal trends of SUHIIs were observed during the day and night (figure 1). The daytime SHUIIs peaked in summer and bottomed in winter for all the regions of China due to the highest and lowest vegetation activity in summer and winter, respectively (Imhoff *et al* 2010, Peng *et al* 2012; Clinton and Gong 2013, Zhou *et al* 2014b). Northeast China experienced the largest seasonal changes of daytime SUHIIs (figure 2), mainly due to the largest seasonal changes of vegetation activity among the three regions. For example, the ΔEVI difference between summer and winter in Northeast China was 2.1 and 1.8 times that in Northwest and Southeast China (data not shown). On the other hand, the nighttime SUHII was the strongest in winter and the weakest in summer/autumn for the northern parts of China (figure 1), possibly due to (a) a more pronounced albedo difference between urban and rural areas during winter than summer because of defoliation and/or snow and ice coverage (Jin *et al* 2005), and (b) a stronger anthropogenic heat flux for building heating and other human activities in urban areas during winter. The nighttime SUHIIs overall remained stable in Southeast China (figure 1), since there was no central-heating system in those cities and the coverage of evergreen vegetation was high. Generally, the seasonal changes of SUHIIs at night were milder than those in the day for all the regions of China (figure 2), possibly because nighttime SUHII was mainly resulted from the larger heat storage capacity of urban surface than rural areas (Oke 1982), which does not change significantly across seasons as compared to vegetation (one major driver for the daytime UHI effect).

4.2. Climate-vegetation control on the diurnal and seasonal patterns

We found a close and positive relationship between mean annual day-night differences of SUHIIs (DNDs) and precipitation (or temperature) (MAP or MAT) across cities (figure 3), confirming the strong contributions of local background climate to the SHUII's spatial patterns found in previous studies (Imhoff

et al 2010, Zhao *et al* 2014). In particular, the positive correlation between daytime SUHIIs and MAT indicates that the daytime SUHIIs are expected to become stronger under a warming climate. The background climate effects in terms of precipitation can be partially explained by soil moisture condition (Oke 1982, Oke *et al* 1991). Soil moisture, with a higher heat capacity, can help store heat during the day for later releasing at night. As a result, the hot–wet cities (i.e., southeastern region), which typically have a larger rural soil moisture content than cold–dry cities (i.e., the Northwest), have higher daytime and lower nighttime SUHIIs and thus larger DNDs. The background climate can also indirectly affect SUHIIs through regulating other variables associated with surface energy balance, such as evapotranspiration (Wang and Dickinson 2012), surface albedo (Hall 2004), and anthropogenic heat emissions (Santamouris *et al* 2001). For example, the humid-hotter regions normally have larger evapotranspiration rates during the daytime in rural areas, which in turn could increase the daytime SUHII by decreasing the sensible heat flux (Oke 1982).

The MAP effects on SUHIIs were weaker in the day than night (figure 3), contrary to a recent report by Zhao *et al* (2014) in North America which showed that the MAP was positively related to daytime SHUII but was not correlated with the nighttime SUHII. Our results are appropriate for China because the daytime SUHII was mainly controlled by the sensible energy partition of the solar radiation (Oke 1982, Oke *et al* 1991), which depends strongly on the vegetation and soil conditions. Both of them were strongly affected by the agricultural practices in China besides climate (Zhou *et al* 2014b, 2015). Further, we showed that the MAP impacts were not linear as observed in North America (Zhao *et al* 2014). Specifically, a quadratic relationship between MAP and mean annual SUHII were observed here in China regardless of SUHII definitions (figures 3 and S7), suggesting that there might be a threshold in terms of local climatic effects on SUHII. For example, the highest daytime SUHII and the lowest nighttime SUHII occurred in cities with MAP around 1000 mm in this analysis (figure 3). Modeling studies are needed to examine the physical mechanisms underlying this non-linear response.

As discussed in section 4.1, vegetation plays a pivotal role in regulating the SUHII patterns due to its cooling effect (Peng *et al* 2012). The results in figure 3 support this mechanism because the difference in enhanced vegetation index between urban and rural areas (i.e., ΔEVI) is negatively and significantly correlated with daytime SUHIIs across cities. In addition, vegetation can substantially influence the SUHII seasonality during the daytime (figure 4), and the effect was especially strong in Northeast China due to the largest seasonal changes of ΔEVI in the region. Vegetation was not found to affect the spatial and seasonal variations of the nighttime SUHIIs (figures 3 and 4), possibly because there was no transpiration at night (Oke 1982, Peng *et al* 2012).

Note that vegetation impacts were usually coupled with those of background climate, since vegetation activities were mainly controlled by the background climate (Nemani *et al* 2003, Piao *et al* 2003). However, the climate couldn't explain all the vegetation cooling effects in China. Human activities and agricultural practices may also play an important role. For example, the cold island effect was observed in one arid city-Lanzhou during the daytime in summer (−2.2 °C) (supporting information figure S6), mostly due to the poorer vegetation condition in rural than urban areas (Zhou *et al* 2014a). In contrast, large daytime SUHII was observed during summer (i.e., 5.2 °C) for another arid city-Yinchuan (supporting information figure S6). This can be explained by the extensive agricultural practice (cultivation and irrigation) (supporting information figure S8) which led to high rural vegetation activity in Yinchuan (Zhou *et al* 2014a). Particularly, cities with double cropping system demonstrated two distinct seasonal SUHII peaks (figure 5), which is another strong evidence for the anthropogenic control on vegetation activities and thus the daytime SUHIIs in China.

4.3. Implications and future efforts

Our findings have three implications. First, it stresses the importance of using time- and site-specific measures to account for UHI effects. Although the SUHII's spatial patterns were significantly controlled by local climate (Zhao *et al* 2014), human activities (e.g., agricultural and urban greening practices) can largely alter the magnitudes of the UHI effects, especially during daytime in summer. Second, it implies that previous studies analyzing SUHII in a single (e.g., daytime in summer or annual mean) or several representative time periods (e.g., summer and winter) might not capture the SUHII's temporal variability. For example, we found that the largest daytime SUHIIs occurred in the spring season rather than the pre-assumed summer for about one-fourth of the cities in China (supporting information figure S6). Hence there is an urgent need to reevaluate the temporal variability of UHI intensity in different climate-vegetation regions. Third, we confirmed that the method used to define UHI matters for the magnitude of UHI (Schwarz *et al* 2011, Zhou *et al* 2015), but will not significantly influence the diurnal and seasonal cycles (supporting information figure S3). This echoes the climate-vegetation control on the SHUII trends over large areas and the robustness of our findings.

However, uncertainties remained and further efforts are needed. First, this study focused on the diurnal and seasonal cycles of the UHI effects. An examination of the inter-annual variability associated with urbanization and climate change would be an

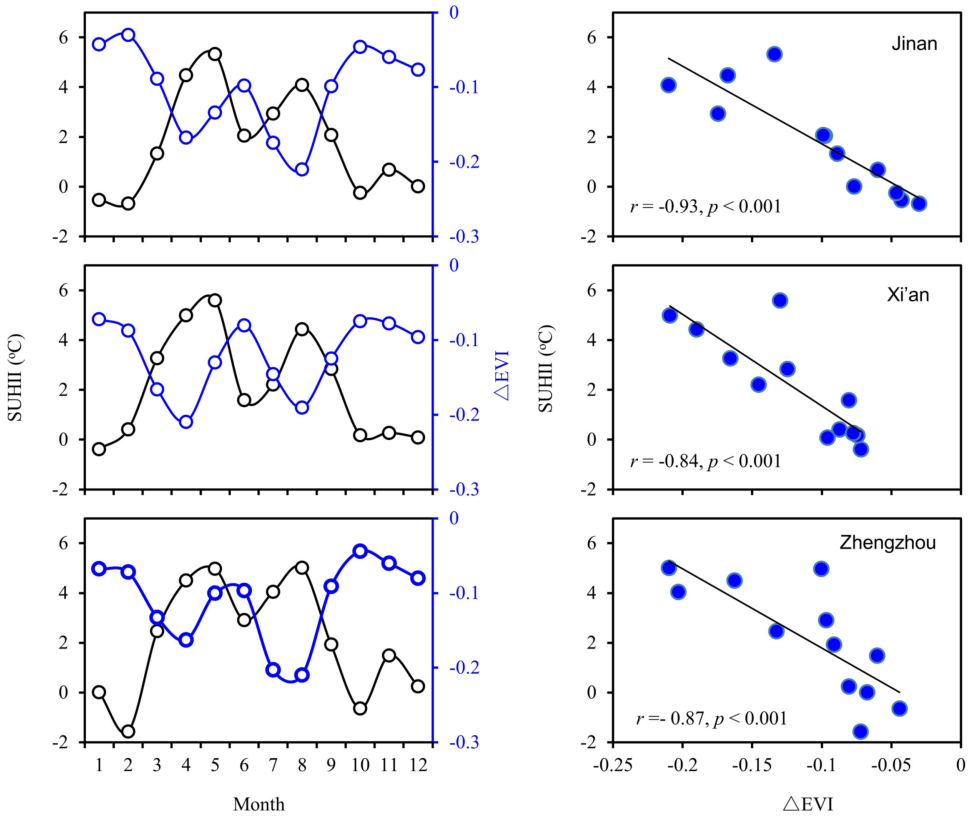

Figure 5. Monthly daytime SUHII (black line) and ΔEVI (blue line) averaged over 2008–2012 for three example cities with double-cropping system (left panels), and their correlations (right panels).

interesting research topic when satellite data over a longer period become available. Second, the surface UHI effect is studied here, the trends of which are different from those of air UHI. In practice, air UHI might be more important in terms of human comfort (Anniballe *et al* 2014), which calls for a comprehensive assessment of both surface and air UHIs in future. Third, the seasonal variations of nighttime SUHIIs were found to be independent of the climate and vegetation seasonality, suggesting that other factors that are not studied here such as surface albedo and anthropogenic heat releases may play more important roles. Moreover, there might be discrepancies between MODIS and ground-based LST measurements and these discrepancies may vary with climate conditions and geographic locations, especially in humid-hot regions (Wan and Dozier 1996). This would invoke uncertainties, which can partially contribute to the diverse seasonal trends of SUHIIs in Southeast China (supporting information figure S6). In addition, all the diurnal and seasonal variations presented in this paper are for clear days. How to convert the clear-day data into whole-sky data (clear and cloudy) remains a challenging research topic (Jin and Dickinson 2010). A combination of direct observations, remote sensing, and numerical modeling is needed for a better understanding of the UHI effects across space (horizontal and vertical) and time in the future.

Acknowledgments

This study was supported by the National Natural Science Foundation of China (#41501465), the Natural Science Foundation of the Jiangsu Higher Education Institutions of China (#15KJB170013), and the Startup Foundation for Introducing Talent of NUIST (2014r051). Funding for the visit of the USDA Forest Service is provided by China Scholarship Council.

References

Angel S, Parent J, Civco D L, Blei A and Potere D 2011 The dimensions of global urban expansion: estimates and projections for all countries 2000–2050 *Progress in Planning* **75** 53–107

Anniballe R, Bonafoni S and Pichierri M 2014 Spatial and temporal trends of the surface and air heat island over Milan using MODIS data *Remote Sens. Environ.* **150** 163–71

Arnfield A J 2003 Two decades of urban climate research: a review of turbulence exchanges of energy and water and the urban heat island *Int. J. Climatol.* **23** 1–26

Chow W T L and Roth M 2006 Temporal dynamics of the urban heat island of Singapore *Int. J. Climatol.* **26** 2243–60

Clinton N and Gong P 2013 MODIS detected surface urban heat islands and sinks: global locations and controls *Remote Sens. Environ.* **134** 294–304

Fast J D, Torcolini J C and Redman R 2005 Pseudovertical temperature profiles and the urban heat island measured by a temperature datalogger network in Phoenix, Arizona *J. Appl. Meteorol.* **44** 3–13

Gong P, Liang S, Carlton E J, Jiang Q, Wu J, Wang L and Remais J V 2012 Urbanisation and health in China *Lancet* **379** 843–52
Grimm N B, Faeth S H, Golubiewski N E, Redman C L, Wu J, Bai X and Briggs J M 2008 Global change and the ecology of cities *Science* **319** 756–60
Hall A 2004 The role of surface albedo feedback in climate *J. Clim.* **17** 1550–68
Howard L 1833 *Climate of London Deduced From Metrological Observations* vol 1 (London: Harvey and Dorton)
Huang L, Li J, Zhao D and Zhu J 2008 A fieldwork study on the diurnal changes of urban microclimate in four types of ground cover and urban heat island of Nanjing China *Building and Environment* **43** 7–17
Imhoff M L, Bounoua L, DeFries R, Lawrence W T, Stutzer D, Tucker C J and Ricketts T 2004 The consequences of urban land transformation on net primary productivity in the United States *Remote Sens. Environ.* **89** 434–43
Imhoff M L, Zhang P, Wolfe R E and Bounoua L 2010 Remote sensing of the urban heat island effect across biomes in the continental USA *Remote Sens. Environ.* **114** 504–13
IPCC 2014 *Climate Change: Impacts Adaptation and Vulnerability* (Cambridge: Cambridge University Press)
Jin M, Dickinson R E and Zhang D 2005 The footprint of urban areas on global climate as characterized by MODIS *J. Clim.* **18** 1551–65
Jin M and Dickinson R E 2010 Land surface skin temperature climatology: benefitting from the strengths of satellite observations *Environ. Res. Lett.* **5** 044004
Kolokotroni M, Ren X, Davies M and Mavrogianni A 2012 London's urban heat island: Impact on current and future energy consumption in office buildings *Energy Build.* **47** 302–11
Li D and Bou-Zeid E 2014 Quality and sensitivity of high-resolution numerical simulation of urban heat islands *Environ. Res. Lett.* **9** 055001
Li D and Bou-Zeid E 2013 Synergistic interactions between urban heat islands and heat waves: The impact in cities is larger than the sum of its parts *J. Appl. Meteorol. Clim.* **52** 2051–64
Li D, Bou-Zeid E and Oppenheimer M 2014 The effectiveness of cool and green roofs as urban heat island mitigation strategies *Environ. Res. Lett.* **9** 055002
Li D, Sun T, Liu M, Yang L, Wang L and Gao Z 2015 Contrasting responses of urban and rural surface energy budgets to heat waves explain synergies between urban heat islands and heat waves *Environ. Res. Lett.* **10** 054009
Manley G 1958 On the frequency of snowfall in metropolitan England *Q. J. R. Meteorol. Soc.* **84** 70–2
Miao S, Chen F, LeMone M A, Tewari M, Li Q and Wang Y 2009 An observational and modeling study of characteristics of urban heat island and boundary layer structures in Beijing *J. Appl. Meteorol. Clim.* **48** 484–501
Motulsky H and Christopoulos A 2004 *Fitting Models to Biological Data Using Linear and Nonlinear Regression: a Practical Guide to Curve Fitting* (Oxford: Oxford University Press)
Nemani R R, Keeling C D, Hashimoto H, Jolly W M, Piper S C, Tucker C J, Myneni R B and Running S W 2003 Climate-driven increases in global terrestrial net primary production from 1982 to 1999 *Science* **300** 1560–3
Oke T R 1973 City size and the urban heat island *Atmospheric Environment* **7** 769–79
Oke T R 1982 The energetic basis of the urban heat island *Q. J. R. Meteorol. Soc.* **108** 1–24
Oke T, Johnson G, Steyn D and Watson I 1991 Simulation of surface urban heat islands under 'ideal' conditions at night:2. Diagnosis of causation *Bound.-Layer Meteorol.* **56** 339–58
Patz J A, Campbell-Lendrum D, Holloway T and Foley J 2005 A Impact of regional climate change on human health *Nature* **438** 310–7
Peng S, Piao S, Ciais P, Friedlingstein P, Ottle C, Bréon F M, Nan H, Zhou L and Myneni R B 2012 Surface urban heat island across 419 global big cities *Environ. Sci. Technol.* **46** 696–703
Peterson T C 2003 Assessment of urban versus rural *in situ* surface temperatures in the contiguous United States: No difference found *J. Clim.* **16** 2941–59
Piao S, Fang J, Zhou L, Guo Q, Henderson M, Ji W, Li Y and Tao S 2003 Interannual variations of monthly and seasonal normalized difference vegetation index (NDVI) in China from 1982 to 1999 *J. Geophys. Res.* **108** 4401
Reid W V 1998 Biodiversity hotspots *Trends Ecol. Evol.* **13** 275–80
Rigo G, Parlow E and Oesch D 2006 Validation of satellite observed thermal emission with *in situ* measurements over an urban surface *Remote Sens. Environ.* **104** 201–10
Roth M, Oke T and Emery W 1989 Satellite-derived urban heat islands from three coastal cities and the utilization of such data in urban climatology *Int. J. Remote Sens.* **10** 1699–720
Santamouris M, Papanikolaou N, Livada I, Koronakis I, Georgakis C, Argiriou A and Assimakopoulos D 2001 On the impact of urban climate on the energy consumption of buildings *Sol. Energy* **70** 201–16
Schneider A, Friedl M A and Potere D 2009 A new map of global urban extent from MODIS satellite data *Environ. Res. Lett.* **4** 044003
Schwarz N, Lautenbach S and Seppelt R 2011 Exploring indicators for quantifying surface urban heat islands of European cities with MODIS land surface temperatures *Remote Sens. Environ.* **115** 3175–86
Seto K C, Fragkias M, Güneralp B and Reilly M K 2011 A meta-analysis of global urban land expansion *PLoS ONE* **6** e23777
Seto K C, Güneralp B and Hutyra L R 2012 Global forecasts of urban expansion to 2030 and direct impacts on biodiversity and carbon pools *Proc. Natl Acad. Sci. USA* **109** 16083–8
Shepherd J M 2005 A review of current investigations of urban-induced rainfall and recommendations for the future *Earth Interactions* **9** 1–27
Storey J, Scaramuzza P, Schmidt G and Barsi J 2005 Landsat 7 scan line corrector-off gap filled product development *Proc. of Pecora* pp 23–7
Tran H, Uchihama D, Ochi S and Yasuoka Y 2006 Assessment with satellite data of the urban heat island effects in Asian mega cities *Int. J. Appl. Earth Observation and Geoinformation* **8** 34–48
United Nations 2015 *Department of Economic and Social Affairs Population Division World Urbanization Prospects* The 2014 revision (New York: United Nations)
Voogt J A and Oke T R 2003 Thermal remote sensing of urban climates *Remote Sens. Environ.* **86** 370–84
Wan Z 2008 New refinements and validation of the MODIS land-surface temperature/emissivity products *Remote Sens. Environ.* **112** 59–74
Wan Z and Dozier J 1996 A generalized split-window algorithm for retrieving land-surface temperature from space *IEEE Transactions on Geoscience and Remote Sensing* **34** 892–905
Wang K and Dickinson R E 2012 A review of global terrestrial evapotranspiration: Observation, modeling, climatology, and climatic variability *Rev. Geophys.* **50** RG2005
Wu J 2015 Urban ecology and sustainability: the state-of-the-science and future directions *Landsc. Urban Plann.* **125** 209–21
Wu S, Yin Y, Zheng D and Yang Q 2005 Aridity/humidity status of land surface in China during the last three decades *Science in China Series D: Earth Sciences* **48** 1510–8
Zhang P, Imhoff M L, Wolfe R E and Bounoua L 2010 Characterizing urban heat islands of global settlements using MODIS and nighttime lights products *Can. J. Remote Sens.* **36** 185–96
Zhao L, Lee X, Smith R B and Oleson K 2014 Strong contributions of local background climate to urban heat islands *Nature* **511** 216–9
Zhao S, Zhou D, Zhu C, Qu W, Zhao J, Sun Y, Huang D, Wu W and Liu S 2015a Rates and patterns of urban expansion in China's 32 major cities over the past three decades *Landsc. Ecol.* **30** 1541–59

Zhao S, Zhou D, Zhu C, Sun Y, Wu W and Liu S 2015b Spatial and temporal dimensions of urban expansion in China *Environ. Sci. Technol.* **49** 9600–9

Zhou B, Rybski D and Kropp J P 2013 On the statistics of urban heat island intensity *Geophys. Res. Lett.* **40** 5486–91

Zhou D, Zhao S, Liu S and Zhang L 2014a Spatiotemporal trends of terrestrial vegetation activity along the urban development intensity gradient in China's 32 major cities *Sci. Total Environ.* **488** 136–45

Zhou D, Zhao S, Liu S, Zhang L and Zhu C 2014b Surface urban heat island in China's 32 major cities: spatial patterns and drivers *Remote Sens. Environ.* **152** 51–61

Zhou D, Zhao S, Zhang L, Sun G and Liu Y 2015 The footprint of urban heat island effect in China *Sci. Rep.* **5** 1–11

Zhou D, Zhao S, Zhang L and Liu S 2016 Remotely sensed assessment of urbanization effects on vegetation phenology in China's 32 major cities *Remote Sens. Environ.* **176** 272–81